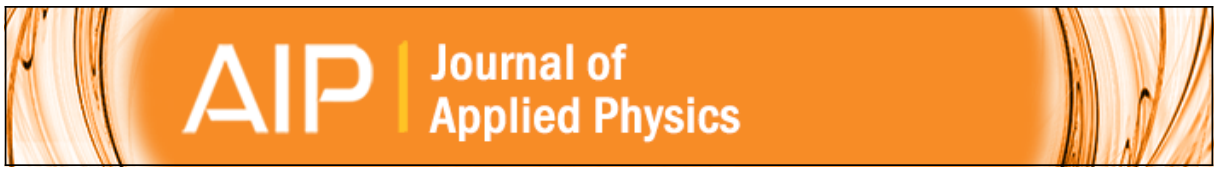

Structural change in polar nanoregion in alkali niobate added Pb(Zn1/3Nb2/3)0.95Ti0.05O3 single crystal and its effect on ferroelectric properties

Jong-Sung Park, Youngsoo Jung, and Jung-Kun Lee

Citation: Journal of Applied Physics **112**, 074109 (2012); doi: 10.1063/1.4757620

View online: http://dx.doi.org/10.1063/1.4757620

View Table of Contents: http://scitation.aip.org/content/aip/journal/jap/112/7?ver=pdfcov

Published by the AIP Publishing

Structural change in polar nanoregion in alkali niobate added $Pb(Zn_{1/3}Nb_{2/3})_{0.95}Ti_{0.05}O_3$ single crystal and its effect on ferroelectric properties

Jong-Sung Park,[1] Youngsoo Jung,[2] and Jung-Kun Lee[2,a)]
[1]*Department of Material Science and Engineering, Myongji University, Yongin, Gyeonggi-do 449-728, Korea*
[2]*Department of Mechanical Engineering and Materials Science, University of Pittsburgh, Pittsburgh, Pennsylvania 15261, USA*

(Received 14 December 2011; accepted 5 September 2012; published online 4 October 2012)

$Pb(Zn_{1/3}Nb_{2/3})_{0.95}Ti_{0.05}O_3$ (PZNT) single crystals with 5 mol. % alkali niobate such as $LiNbO_3$ (LN), $NaNbO_3$ (NN), and $KNbO_3$ (KN) were fabricated by using a flux method to investigate the effect of A-site cation radius on the structure and ferroelectric properties of PZNT under electric field (E-field). Their structure and properties showed different electric field dependence. Polarization versus electric field and strain versus electric field curves of PZNT-0.05LN showed E-field induced phase transition from a relaxor state to a normal ferroelectric state. However, only relaxor behavior was observed in PZNT-0.05NN and PZNT-0.05KN. The effect of A-site ion doping is attributed to the change in local lattice distortion and polar nano-region. When smaller cation such as Li ion substitutes Pb ion, the off-center displacement of Nb ion stabilizes rhombohedral lattice distortion. They, in turn, facilitate the development of macro-domains under electric field (E-field) in PZNT-0.05LN. In contrast, the substitution of Pb with larger cations such as Ni and K decreases the rhombohedral distortion of PZNT, which leads to the disappearance of unique E-field induced phase transition from rhombohedral to tetragonal phase in PZNT. Therefore, non-linear electrostrictive behavior of relaxor ferroelectrics is found in PZNT-0.05NN and PZNT-0.05KN. © *2012 American Institute of Physics*. [http://dx.doi.org/10.1063/1.4757620]

I. INTRODUCTION

$Pb(Zn_{1/3}Nb_{2/3})_{0.95}Ti_{0.05}O_3$ (PZNT) is one of relaxor ferroelectrics that shows superior electromechanical properties.[1–5] When electric field (E-field) is applied along [001] direction of PZNT single crystal, the crystal expands up to 1%.[1] Such a large strain is explained by E-field induced phase transition (EIPT). As E-field applied to the crystal reaches ~20 kV/cm, PZNT crystal shows the phase transition from rhombohedral structure to tetragonal structure, which causes an abrupt change in polarization versus E-field (P-E) and strain versus E-field (S-E) curves.[1]

Unique ferroelectric properties of relaxor ferroelectrics such as large electrostriction, diffuse phase transition, and large dielectric constant are correlated with the polar nano-regions (PNRs) and the chemically ordered regions (CORs).[6] CORs in PZN result from the ordered arrangement of Zn and Nb cations, which is explained by the charge balanced random-layer model.[7] Such CORs showed the rhombohedral distortion driven by large polarizability of Pb and large ionic size difference between Zn and Nb.[8,9] Rhombohedral distortion in CORs is one of origins for PNRs, though the exact relation between CORs and PNRs is still under investigation.[9–13]

The growth, alignment, and interconnection of PNRs by temperature or electric field (E-field) form a macro-polar domain with long range polarization.[11] In PZNT crystals with a rhombohedral structure, the application of E-field reorients the rhombohedral domains and results in the pseudotetragonal symmetry.[14]

It is known that an A-site cation in the perovskite structure influences the formation of CORs and PNRs.[9] We recently demonstrated that the addition of the $NaNbO_3$ or $KNbO_3$ into PZNT polycrystals controls the thermodynamic stability and ferroelectricity of PZNT. This is due to the change in a tolerance factor (t), which could be described by

$$t = \frac{R_A + R_O}{\sqrt{2}(R_B + R_O)}, \quad (1)$$

where each of R_A, R_B, and R_O is the ionic radius of A-site cation, B-site cation, and oxygen ion in ABO_3 perovskite structure, respectively.[15,16] However, low thermodynamic stability of PZNT with small tolerance factor and difficulty in growing single crystals has prevented further study on the unique features of PZNT based solid solutions. The effect of alkali niobate doping on the structure of PNRs, the long range ferroelectric domain, and the E-field induced phase transition is not well understood yet. In this study, we grew $(1-x)Pb(Zn_{1/3}Nb_{2/3})_{0.95}Ti_{0.05}O_3-xRNbO_3$ (PZNT-RN; R = Li, Na, K) single crystals and systematically investigated the effect of A-site cation on the crystal structure, ferroelectric domains, local polarization, and long-range polarization of PZNT.

a)Author to whom correspondence should be addressed. E-mail: jul37@pitt.edu. Tel.: +1-412-648-3395. FAX: +1-412-624-8069.

II. EXPERIMENTAL PROCEDURES

A. Growth of single crystals

$Pb(Zn_{1/3}Nb_{2/3})_{0.95}Ti_{0.05}O_3$ (PZNT) crystal and RN added PZNT crystals were grown using the high temperature flux technique. The compositions of RN added PZNT crystals are (95-*x*)% $Pb(Zn_{1/3}Nb_{2/3})O_3$ (PZN) – 5% $PbTiO_3$ (PT) – *x*% $LiNbO_3$ (PZNT-*x*LN), (95-*x*)% PZN – 5% PT – *x*% $NaNbO_3$ (PZNT-*x*NN) and (95-*x*)% PZN – 5% $PbTiO_3$ – *x*% $LiNbO_3$ (PZNT-*x*KN), where *x* is 0.025 and 0.05. Reagent grade Pb_3O_4 (Sigma-Aldrich, USA), ZnO (High Purity Chemicals, Japan), Nb_2O_5 (High Purity Chemicals, Japan), Li_2CO_3 (Merck, USA), K_2CO_3 (Junsei Chemical, Japan), Na_2CO_3 (Wako Chemical, Japan), and TiO_2 (High Purity Chemicals, Japan) powders were used. Raw powders were weighed with excess Pb_3O_4 and alkali carbonate as flux. The molar ratio of flux Pb_3O_4 to stoichiometric Pb_3O_4 was 6:4, and the molar ratio of the flux alkali carbonate to stoichiometric alkali carbonate used to modify the PZNT was 0.2:1.

Raw materials were weighed and mixed with the alcohol for 24 h using a ball mill. Excess Pb_3O_4 and alkali carbonate powder were added to form a flux at high temperature. The mixed powders were loaded into a platinum crucible, which was placed in an alumina crucible sealed in air with an alumina lid and alumina cement to minimize PbO volatilization. The loaded crucible was held at a soak temperature of 1250 °C for 10 h. After soaking, the furnace was cooled slowly at a rate of 1 °C/h to 920 °C for the growth of single crystals followed by furnace-cooling to room temperature to prevent a formation of a pyrochlore secondary phase. Non-crystallized solid in the crucible was washed out by hot HNO_3. The size of separated crystals ranged from 3 to 25 mm.

B. Characterization of single crystals

After single crystals were ground into fine powders, the crystal structure of powders was examined by x-ray diffraction (XRD). Nominal compositions of the single crystals were confirmed by inductively coupled plasma-atomic emission spectrometer (ICP-AES, Model: ICPS-1000IV, Shimadzu, Japan).

To measure the ferroelectric properties of single crystals, we found [001] direction of the crystals by a back reflection Laue method. After the crystallographic orientation was determined, samples were prepared by polishing using silicon carbide and diamond paste. For electrical characterization, plate shape samples with thickness of 0.4–0.5 mm were prepared, and platinum electrodes were sputtered on flat faces. E-field ranging from 0 to 70 kV/cm was applied to the samples using a high voltage amplifier (Model: 609 E-6, Trek, USA). The frequency of E-field was 0.2 Hz. P-E curve was measured by a modified Sawyer–Tower circuit. S-E curve was also obtained by linear variable differential transducer (LVDT). To increase the resolution of LVDT, the signal was detected through a lock-in amplifier (Model: AX1.0 S, Solartron, UK).

The domain configuration of the crystals was observed by a polarized microscope with a crossed Nicol prism. For *in-situ* domain study under E-field, cubes with {001} faces were prepared, and the platinum electrode with the thickness of ~20 nm was sputtered on parallel faces of the cubes. Then, E-field was applied to the platinum electrodes, and the change in the domain configuration was probed through transparent electrodes.

To study the local polarization at micro-scale, Raman spectra of PZNT-RN crystals with {001} face were taken by a confocal micro-Raman spectrometer (Model: NIS3100, Jasco, Japan) in a backscattering geometry. Measurements were performed in crossed Y(XZ)\Y and parallel Y(ZZ)\Y polarization configurations in which X, Y, and Z represented the ⟨001⟩ family directions in a pseudo-cubic crystal structure.

TABLE I. Results of ICP analysis on the content of alkali elements (Li^+, Na^+, or K^+) in A-site, Nb and Ti in B-site.

	Theoretical value	PZNT-KN	PZNT-NN	PZNT-LN
R/A-site	0.050	0.052	0.051	0.043
Nb/B-site	0.684	0.676	0.681	0.703
Ti/B-site	0.050	0.051	0.051	0.050

III. RESULTS

Table I summarizes the result of ICP analysis on the compositions of PZNT-RN crystals. The content of alkali elements, Nb, and Ti is in agreement with theoretical expectations. This confirms that alkali niobates such as $LiNbO_3$, $NaNbO_3$, and $KNbO_3$ formed a complete solid solution with PZNT when the crystals were grown.

Figure 1 shows XRD patterns of PZNT-0.05LN, PZNT-0.05NN, and PZNT-0.05KN crystals. There was no split of (002) peak, which indicates that three crystals maintain the rhombohedral structure of PZNT or pseudo cubic structure.[1,17,18] In addition to the fundamental peaks of the perovskite structure, no additional peaks associated with the second phase were found in Fig. 1.[19]

Figure 2 shows bipolar P-E and S-E curves of PZNT-0.05LN, PZNT-0.05NN, and PZNT-0.05KN single crystals along [001] direction. Remanent polarization (P_r), saturated

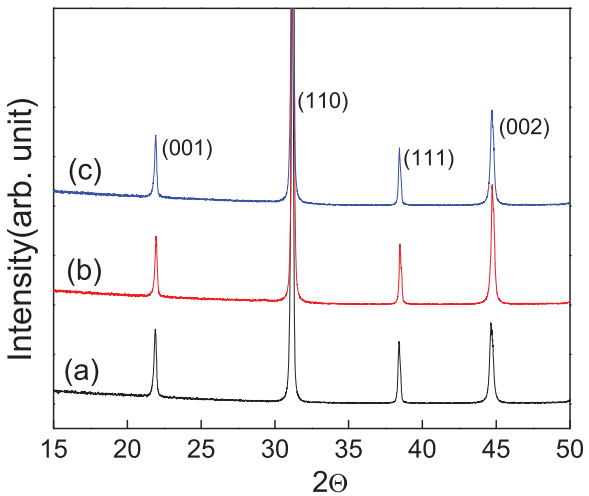

FIG. 1. XRD patterns of (a) PZNT-LN, (b) PZNT-NN, and (c) PZNT-KN.

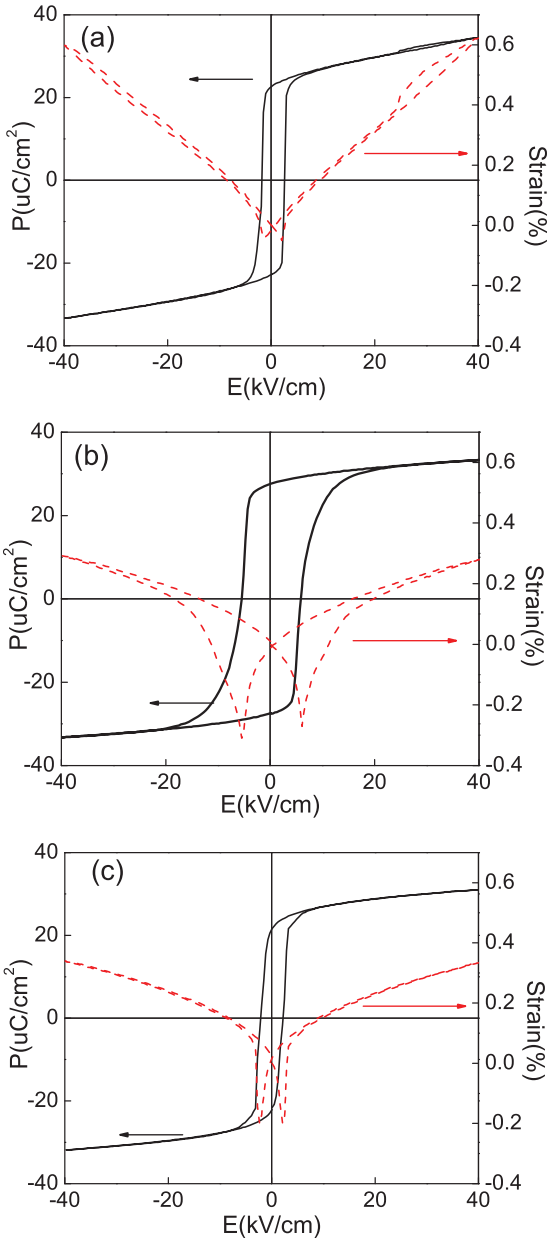

FIG. 2. Bipolar P-E and S-E curves of [001] oriented (a) PZNT-LN, (b) PZNT-NN, and (c) PZNT-KN single crystals.

polarization (P_s), and coercive field (E_c) of the crystals are summarized in Table II. E_c of three crystals are between 2.2 and 5.6 kV/cm, which is comparable to E_c of PZNT (~2.7 kV/cm).[1] But a polarization of PZNT-0.05KN decreased more steeply around a zero field, which increased a difference between P_r and P_s. This is summarized in Table II. Addition of different alkali niobate also changed S-E curves of single crystals. Strain at E-field of 40 kV/cm was about 0.6% for PZNT-LN while this was 0.28% for PZNT-NN and 0.33% for PZNT-KN, respectively.

TABLE II. The remnant polarization (P_r), saturated polarization (P_s), and coercive field (E_c) of PZNT-RN single crystals along [001] direction.

	PZNT-LN	PZNT-NN	PZNT-KN
Pr ($\mu C/cm^2$)	22.7	27.6	21.2
Ps ($\mu C/cm^2$)	24.3	29.8	26.9
Ps-Pr ($\mu C/cm^2$)	1.6	2.2	5.7
Ec (kV/cm)	2.6	5.6	2.2

To understand the correlation between strain and polarization, strains vs. polarization curves (S-P curves) of PZNT-0.05LN, PZNT-0.05NN, and PZNT-0.05KN, which are deduced from S-E and P-E, are plotted in Fig. 3. Relaxor ferroelectrics show an electrostrictive behavior, which can be described by

$$x_3 = Q_{33}P_3^2, \tag{2}$$

where x_3, Q_{33}, and P_3 are the strain, the electrostrictive constant, and the polarization in unique 3-direction, respectively. On the other hand, the electrostrictive relationship of normal ferroelectric materials can be described by

$$x_3 = d_{33}E_3, \tag{3}$$

where d_3 and E_3 are a piezoelectric constant and an E-field applied along unique 3-direction.[15] S-P curve of PZNT-0.05KN is well fitted with a quadratic relation in Eq. (1) while that of PZNT-0.05LN and PZNT-0.05NN deviates from the quadratic relation. With smaller E_c and P_r, the quadratic S-P curve indicates that the addition of KN into PZNT leads to the appearance of a typical relaxor ferroelectrics. A similar trend was found in PZNT-0.05KN ceramics prepared by a solid state reaction.[15]

Figure 4 shows the unipolar S-E curves of [001] oriented PZNT and PZNT-0.05LN single crystals. Unipolar S-E curves of PZNT and PZNT-0.05LN consist of three parts. A relatively linear change in S-E curve at low E-field corresponds to the strain of a rhombohedral structure. In PZNT, an intricate change of S-E curve in the intermediate E-field regime is attributed to EIPT from the rhombohedral structure to the tetragonal structure. Once the transition to the tetragonal structure is completed, a linear relation between strain and E-field reappeared. In a rhombohedral region, an average piezoelectric constant of PZNT-0.05LN can be calculated from the slope of S-E curve. The piezoelectric constant of PZNT-0.05LN is 1650 pC/N, which is equal to that of PZNT.

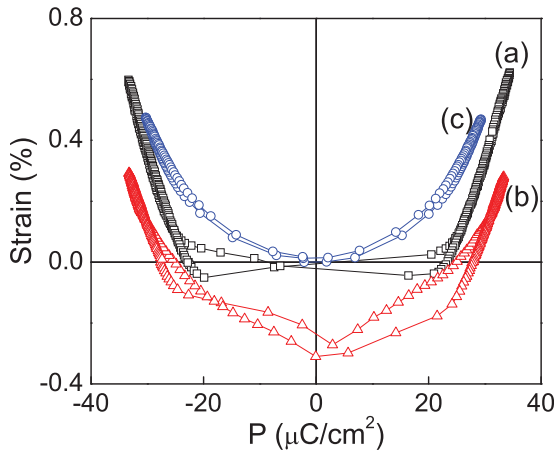

FIG. 3. Strains vs. polarization curves (S-P curves) of (a) PZNT-LN, (b) PZNT-NN, and (c) PZNT-KN.

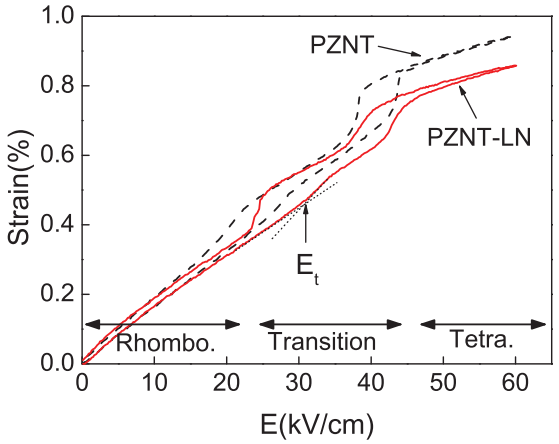

FIG. 4. Unipolar S-E curves of [001] oriented PZNT and PZNT-LN single crystals.

In a phase transformation region, the threshold E-field for EIPT (E_{PT}) was determined from the boundary of linear regime of S-E curve. E_{PT} was 22 kV/cm for PZNT and 32 kV/cm for PZNT-0.05LN. In the middle of EIPT, S-E curves showed a hump, which could be explained by a two-step phase transition. As E-field is applied to the crystals along [001] direction, the [111] polarization vector of rhombohedral structure rotates gradually until the polarization vector is aligned to [001] direction. When the polarization vector is placed along [110] direction during this gradual rotation, the local energy minimum condition is satisfied, and the atomic lattice has an orthorhombic symmetry.[14] Further increase in E-field transforms the orthorhombic symmetry to the tetragonal symmetry. Therefore, there are two sequential phase transitions, i.e., a rhombohedral to orthorhombic transition and an orthorhombic to tetragonal transition. In the tetragonal region, the slope of the S-E curve is nearly same in PZNT and PZNT-0.05LN; however, the absolute value of the stain was 10% lower for PZNT-0.05LN than for PZNT. This indicates that the lattice parameter along the c-axis of a transformed tetragonal structure of PZNT-0.05LN is smaller than that of PZNT due to the substitution of a smaller Li^{+1} cation.

Fig. 5 shows the unipolar P-E and S-E curves of [001] oriented PZNT-0.05LN, PZNT-0.05NN, and PZNT-0.05KN single crystals. It is noted that E-field dependent properties of PZNT-0.05NN and PNZT-0.05KN are different from those of PZNT-0.05LN. In contrast to PZNT-LN, a steep and complicated change is not observed in P-E and S-E curves of PZNT-KN and PZNT-NN. Only PZNT-LN displayed a hysteresis in middle of P-E and S-E curves. This indicates that the crystal structure of PZN-KN and PZN-NN do not experience the phase transition under E-field.

To further trace the effects of NN substitution on EIPT, we decreased the amount of NN in PZNT from 5 mol. % to 2.5 mol. %. Figure 6 shows S-E and P-E curves of PZNT-0.025NN and PZNT-0.05NN. Addition of 2.5 mol. % NN decreases E_{PT} from 22 to 12 kV/cm and increases d_{33} of the rhombohedral region from 1650 pC/N to 3500 pC/N. When the amount of NN reaches 5 mol. %, the evidence of EIPT was not found in S-E curve and d_{33} of the rhombohedral region decreased from 3500 pC/N to 1150 pC/N. Such an

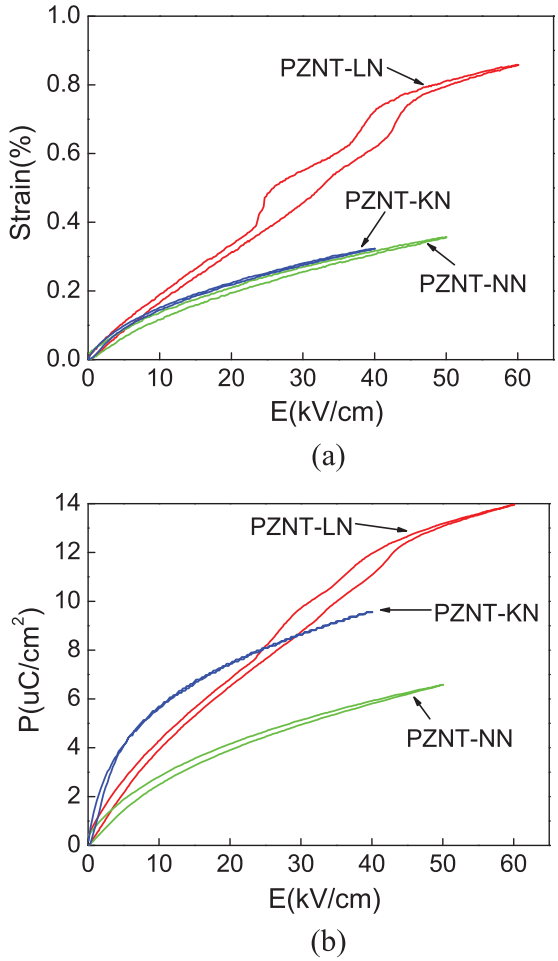

FIG. 5. Unipolar (a) P-E and (b) S-E curves of [001] oriented PZNT-LN, PZNT-NN, and PZNT-KN single crystals.

effect of NN addition on EIPT was found even in P-E curves of PZNT-0.025NN. In Fig. 6(b), the intricate two-step phase transition was not observed, and E_{PT} was decreased to 6 kV/cm. Then, EIPT disappeared in P-E curve of PZNT-0.05NN.

Figure 7 shows optical micrographs of PZNT-0.05LN under polarized light. During the examination, E-field was applied along the ⟨001⟩ direction of the crystals. Before E-field is applied, no ferroelectric domain was observed. However, at an E-field of 25 kV/cm, normal ferroelectric domains were found in PZNT-0.05LN. The domain boundaries in Fig. 7(b) were parallel to {110} planes, which is observed in normal ferroelectrics with the rhombohedral or tetragonal symmetry. Given that the rhombohedral to tetragonal transition occurred at E-field of about 30 kV/cm, this indicates that E-field aligned polar regions with the rhombohedral symmetry and formed the macroscopic polar region.[20] Fig. 7(c) shows an optical micrograph of PZNT-0.05NN when E-field of 20 kV/cm was applied along the ⟨001⟩ direction. Colorful fringes and macro-scale domains of normal ferroelectrics were not observed in the optical micrograph of PZNT-0.05NN. This is consistent with S-E and P-E curves of PZNT-0.05NN that showed the electrostrictive behavior of typical relaxor ferroelectrics.

Figure 8 shows Raman spectra of PZNT, PZNT-0.025NN, and PZNT-0.05NN crystals before they were

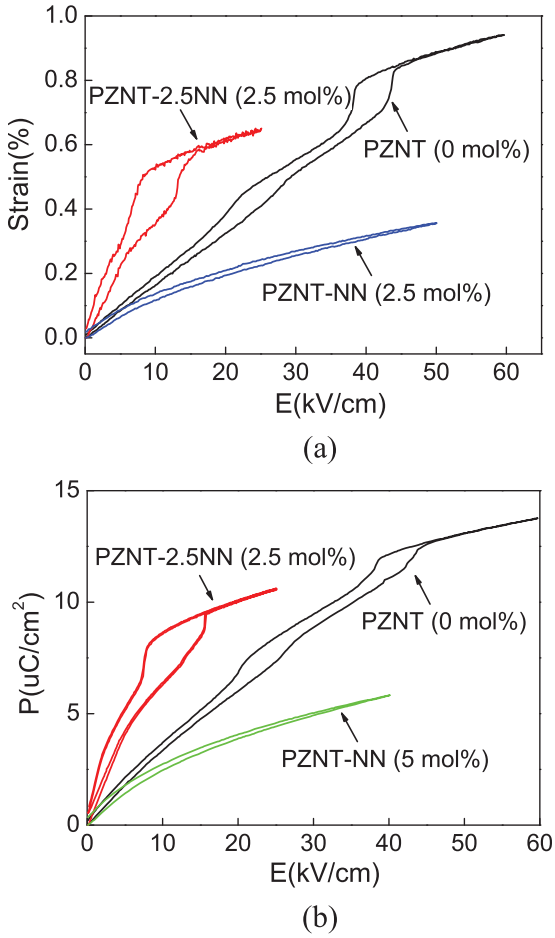

FIG. 6. (a) S-E curves and (b) P-E curves of (1-x) PZNT + x NN (x = 0, 0.025, and 0.05).

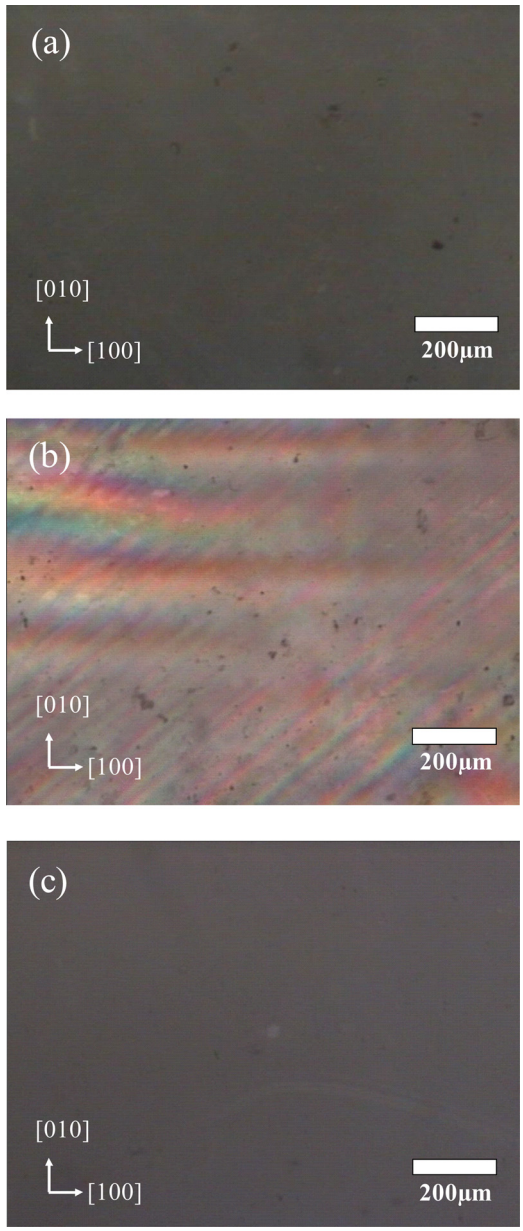

FIG. 7. Optical micrographs of PZNT-LN (a) before applying an E-field and (b) upon applying an E-field of 25 kV/cm along the ⟨001⟩ direction, and an optical micrograph of PZNT-NN upon applying an E-field of 20 kV/cm along the ⟨001⟩ direction.

exposed to E-field. The measurements were conducted in crossed (XZ) and parallel (ZZ) polarization configurations. Raman peaks in Fig. 8 are traced to the asymmetric ionic displacement of the rhombohedral phase (R3m) and the COR with a space group of $Fm\bar{3}m$.[21,22] It is noted that Raman spectra peaks exhibit different configuration dependence. A strong mode near 780 cm^{-1} represents the stretching of Zn-O-Nb bond (A_{1g}).[21] In PZNT, the A_{1g} mode could be detected clearly in both of XZ and ZZ configuration. However, in PZNT-0.025NN and PZNT-0.05NN, XZ configuration makes A_{1g} mode weaker than XZ configuration. A depolarization ratio (Ixz/Izz) of A_{1g} mode obtained from integrated intensities in XZ and ZZ polarized Raman spectra are summarized in Fig. 9. The depolarization ratio decreased with increasing the amount of NN in PZNT from 0 to 0.05 mol. %. Such an abrupt decrease in the depolarization ratio was found in relaxor ferroelectrics when the symmetry of long range polarization changes from the rhombohedral one to the tetragonal one.[22,23] Therefore, the depolarization ratio of PZNT-NN indicates that the small amount of NN facilitates the phase transition from the rhombohedral structure to the tetragonal one.

IV. DISCUSSION

Though a small amount of RN is added to PZNT, PZNT-0.05LN, PZNT-0.05NN, and PZNT-0.05KN show different ferroelectric behaviors. When E-field is applied to PZNT-0.05LN crystal, the macro-scale ferroelectric domains appeared, and the two-step phase transition to the tetragonal structure occurred. E_{PT} of PZNT-0.05LN is even higher than that of PZNT, which means that the ferroelectric rhombohedral phase persists up to higher E-field. On the contrary, PZNT-0.05NN and PZNT-0.05KN crystals do not show EIPT and macro-scale ferroelectric domains when E-field is applied. Also, S-E and P-E curves indicate that PZNT-0.05NN and PZNT-0.05KN possess the electrostrictive behavior of typical relaxor ferroelectrics at room temperature.

Raman spectra show that the enhancement of normal ferroelectric properties in PZNT-0.05LN and the appearance of relaxor ferroelectric properties in PZNT-0.05NN and PZNT-0.05KN are correlated with the change in the

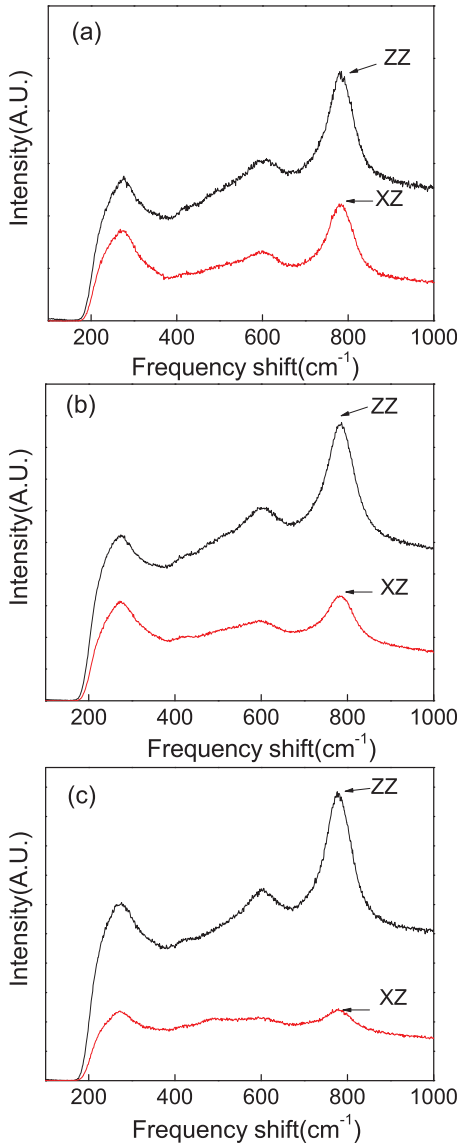

FIG. 8. Raman spectra of (a) PZNT, (b) PZNT-0.025NN, and (c) PZNT-0.05NN measured in crossed (XZ) and parallel (ZZ) polarization before applying the E-field.

structure of the polar region. In ferroelectric materials, a part of cation is off-centered to produce permanent dipoles. Such off-centering of cation occurs through the decoupling of ferroelectric cations from neighbor cations. In PNRs of PZN-based crystals, a size difference between Zn and Nb cations shifts Pb cation along ⟨111⟩ direction toward larger Zn cation and places the lone pair electron of Pb between Pb and Zn cation.[8] This, in turn, leads to the off-centering of Nb cation, which is responsible for the local polarization of PNRs.

The distortion in the alkali niobate added PZN is influenced by the electric charge and size of A-site cation dopant. Since the charge of Li, K, and Na ions is same, the different effect of alkali niobate doping is mainly attributed to the size of doped cations. The appearance of E-field induced phase transition in PZN-0.05LN shows that smaller Li ion shifts Pb and Nb cations along ⟨111⟩ direction more than K and Na and stabilizes the rhombohedral distortion. In other words, the smaller tolerance factor of $LiNbO_3$ promotes the tilting

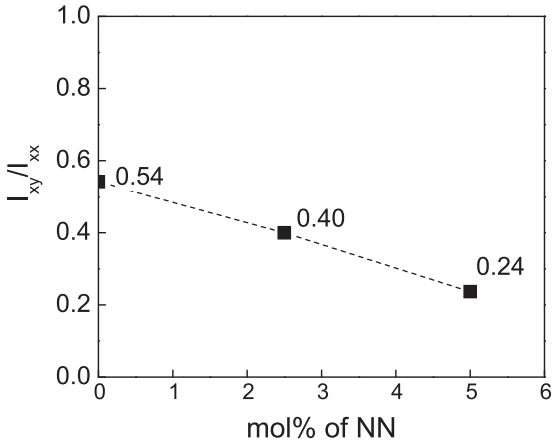

FIG. 9. Depolarization ratios (Ixz/Izz) calculated by peak intensity ratios of A_{1g} modes in XZ and ZZ polarized Raman spectra of PZNT, PZNT-0.025NN, and PZNT-0.05NN.

of oxygen octahedral and produces the local polarization with the rhombohedral symmetry.[24]

The other effect of adding the RN into PZNT is the increase of concentration of Nb cation in B-site. This can also decrease the coupling of Pb with Zn because the difference in the ionic size between Zn and Nb is one of the driving forces to make the strong coupling of Pb with Zn. This also resulted in the decrease of rhombohedral distortion with increasing the amount of NN. Such decrease of rhombohedral distortion induces the tetragonal phase before the transformation to cubic phase, which can be found with increasing temperature.[23] Such transformation to tetragonal phase by adding NN into PZNT can explain the absence of EIPT in P-E or S-E curve. And this also resulted in the decrease of depolarization in polarized Raman analysis by increasing the amount of NN.

V. CONCLUSION

5 mol. % of alkali niobate such as $LiNbO_3$, $NaNbO_3$, and $KNbO_3$ was added into PZNT single crystals. The addition of $LiNbO_3$ increased the rhombohedral distortion and facilitated the appearance of normal ferroelectric properties under E-field. On the other hand, the addition of $NaNbO_3$ and $KNbO_3$ suppressed the E-field induced phase transition of PZNT and strengthened the relaxor ferroelectric properties. The effects of alkali niobates are explained by the difference in the size of A-site cations. Smaller size of Li cation stabilizes the rhombohedral distortion of PNRs and provides lager polarization, compared with K and Na cations.

ACKNOWLEDGMENT

The authors thank Hyun-min Park at Korea Research Institute of Standards and Science in South Korea for helping the determination of crystal direction by a back reflection Laue method.

[1]S. E. Park and T. R. Shrout, J. Appl. Phys. **82**, 1804–1811 (1997).
[2]K. K. Rajan, M. J. Zhang, and L. C. Lim, Jpn. J. Appl. Phys., Part 1 **44**, 264–266 (2005).
[3]S. E. Park and T. R. Shrout, IEEE Trans. Ultrason. Ferroelectr. **44**, 1140–1147 (1997).

[4]J. K. Lee, J. Y. Yi, K. S. Hong, and S. E. Park, Jpn. J. Appl. Phys., Part 1 **40**, 6506–6509 (2001).
[5]J. K. Lee, J. Y. Yi, and K. S. Hong, J. Appl. Phys. **96**, 7471–7475 (2004).
[6]D. S. Fu, H. Taniguchi, M. Itoh, S. Koshihara, N. Yamamoto, and S. Mori, Phys. Rev. Lett. **103**, 207601–207604 (2009).
[7]Y. Yan, S. J. Pennycook, Z. Xu, and D. Viehland, Appl. Phys. Lett. **72**, 3145–3147 (1998).
[8]I. W. Chen, P. Li, and Y. Wang, J. Phys. Chem. Solids **57**, 1525–1536 (1996).
[9]N. Setter and L. E. Cross, J. Mater. Sci. **15**, 2478–2482 (1980).
[10]A. A. Bokov and Z. G. Ye, J. Mater. Sci. **41**, 31–52 (2006).
[11]I. K. Jeong, T. W. Darling, J. K. Lee, T. Proffen, R. H. Heffner, J. S. Park, K. S. Hong, W. Dmowski, and T. Egami, Phys. Rev. Lett. **94**, 147602–147605 (2005).
[12]I. K. Jeong, J. K. Lee, and R. H. Heffner, Appl. Phys. Lett. **92**, 172911–172913 (2008).
[13]X. F. Long, A. A. Bokov, Z. G. Ye, W. G. Qu, and X. L. Tan, J. Phys.-Condens. Mater. **20**, 15210–15216 (2008).
[14]H. X. Fu and R. E. Cohen, Nature **403**, 281–283 (2000).
[15]J. S. Park, J. K. Lee, H. M. Park, and K. S. Hong, J. Am. Ceram. Soc. **90**, 3512–3516 (2007).
[16]J. S. Park, J. K. Lee, and K. S. Hong, J. Appl. Phys. **101**, 114101–114107 (2007).
[17]I. Grinberg, M. R. Suchomel, P. K. Davies, and A. M. Rappe, J. Appl. Phys. **98**, 94111–94120 (2005).
[18]J. J. Lima-Silva, I. Guedes, J. Mendes, A. P. Ayala, M. H. Lente, J. A. Eiras, and D. Garcia, Solid State Commun. **131**, 111–114 (2004).
[19]B. K. Kim, S. B. Cha, and J. H. Park, Mater. Sci. Eng. B **58**, 244–250 (1999).
[20]J. K. Lee, J. Y. Yi, K. S. Hong, S. E. Park, and J. Millan, J. Appl. Phys. **91**, 4474–4478 (2002).
[21]P. S. Dobal, R. S. Katiyar, and C. S. Tu, J. Raman Spectrosc. **34**, 152–156 (2003).
[22]A. Lebon, M. El Marssi, R. Farhi, H. Dammak, and G. Calvarin, J. Appl. Phys. **89**, 3947–3954 (2001).
[23]J. Toulouse, F. Jiang, O. Svitelskiy, W. Chen, and Z. G. Ye, Phys. Rev. B **72**, 184106–184117 (2005).
[24]P. M. Woodward, Acta Crystallogr. B **53**, 44–66 (1997).